3,4-Disubstituted derivatives of 1,2,5-thiadiazole 1,1-dioxide. Ethanol addition reactions and electroreduction of 3-methyl-4-phenyl and 3,4-dimethyl derivatives in acetonitrile and ethanol solvents

José Alberto Caram, María Virginia Mirífico, Silvia Lucía Aimone, and Enrique Julio Vasini

Abstract: 3-Methyl-4-phenyl-1,2,5-thiadiazole 1,1-dioxide (**TMP**), as well as 3,4-dimethyl-1,2,5-thiadiazole 1,1-dioxide (**TMM**), react with ethanol (EtOH), which adds to one of their C=N double bonds. The equilibrium constants for the addition reaction are measured in mixed acetonitrile (ACN) – EtOH solvents by means of UV spectroscopy in the case of **TMP**, and by ^{13}C NMR spectroscopy in the case of **TMM**, since **TMM** presents only terminal UV absorption. Both equilibrium constants are also estimated through cyclic voltammetry (CV) experiments. In the case of **TMP**, the ethanol molecule adds to the C=N bond located on the methyl-substituted side of the substrate, according to ^{13}C NMR spectroscopy and CV results. The electroreduction characteristics of the substrates and their ethanol addition products are studied using CV techniques in ACN, EtOH, and ACN–EtOH solvent mixtures. The radical anion formed by the first electron transfer to **TMM** is unstable and decomposes rapidly while that corresponding to **TMP** undergoes a relatively slow homogeneous second-order reaction with the substrate ($k = 3 \times 10^2$ M^{-1} s^{-1}). The equilibrium constant for EtOH addition and the voltammetric properties of the substrates are compared with those of the previously studied 3,4-diphenyl derivative (**TPP**).

Key words: electrochemistry, thiadiazoles, structure–reactivity relations, kinetics.

Résumé : Le 1,1-dioxyde de 3-méthyl-4-phényl-1,2,5,thiadiazole (**TMP**) aussi bien que le 1,1-dioxyde de 3,4-diméthyl-1,2,5-thiadiazole (**TMM**) réagissent avec le méthanol qui s'additionne sur une de leurs doubles liaisons. On a mesuré les constantes d'équilibre de la réaction d'addition dans un mélange d'acétonitrile et d'éthanol comme solvant (ACN)–EtOH, en faisant appel à la spectroscopie UV dans le cas du **TMP** et à la spectroscopie de RMN du ^{13}C dans le cas du **TMM** puisque ce dernier ne présente que des absorptions terminales en UV. On a également évalué les constantes d'équilibre à l'aide d'expériences de voltamétrie cyclique. Dans le cas du **TMP**, la molécule d'éthanol s'additionne sur la double liaison C=N située du côté du méthyle substitué sur le substrat en accord avec les résultats obtenus par spectroscopie de RMN du ^{13}C. Faisant appel aux techniques de CV dans du ACN, EtOH et du ACN–EtOH comme solvants, on a étudié les caractéristiques de l'électroréduction des substrats et de leurs produits résultant de l'addition de l'éthanol. L'anion radicalaire formé lors du premier transfert d'électron vers le **TMM** est instable et se décompose rapidement tandis que le **TMP** correspondant donne avec le substrat, une réaction d'ordre deux homogène relativement lente ($k = 3 \times 10^2$ M^{-1} s^{-1}). On a comparé les constantes d'équilibre de l'addition d'éthanol et les propriétés voltamétriques des substrats avec celles dérivés 3,4-diphényles (**TPP**) étudiés précédemment.

Mots clés : électrochimie, thiadiazoles, relations structure–réactivité, cinétiques.

[Traduit par la rédaction]

Introduction

The 1,1-dioxides of 1,2,5-thiadiazoles belong to a group of heterocycles containing the sulfamide moiety that present interesting chemical properties and a variety of applications as biologically active compounds and as fine chemicals. A detailed review has been written by Aran et al. (1). Several pharmacological uses have been suggested and patented for 1,2,5-thiadiazole 1,1-dioxides, but their chemical properties are largely unexplored and "only a heterogeneous series of generally unrelated reactions are known" (1).

Our previous work has shown, through UV and ^{1}H and ^{13}C NMR spectroscopy (2), that 3,4-diphenyl-1,2,5-thiadiazole 1,1-dioxide (**TPP**) in acetonitrile (ACN) – ethanol (EtOH) solvent mixtures is in equilibrium with the thiadiazoline (3-ethoxy-3,4-diphenyl-1,2,5-thiadiazoline 1,1-dioxide: **TPPH·OEt**) formed through the addition of ethanol to one of its C=N double bonds. The formation equilibrium constant at

Received January 29, 1996.

J.A. Caram, M.V. Mirífico, S.L. Aimone, and E.J. Vasini.[1] Instituto de Investigaciones Fisicoquímicas Teóricas y Aplicadas (INIFTA), Facultad de Ciencias Exactas, Departamento de Química, Universidad Nacional de La Plata, Casilla de Correo 16, Sucursal 4, (1900) La Plata, Argentina.

[1] Author to whom correspondence may be addressed. Telephone: 5.4-21-25-7430 / 7291. Fax: 54-21-25-4642. E-mail: vasini@isis.unlp.edu.ar

25.0°C is 3.3 M^{-1}.[2] Thus **TPP** exists in EtOH solution as the thiadiazoline **TPPH·OEt**.

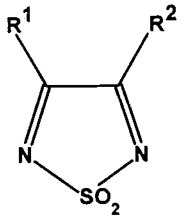

$R^1 = R^2 = Ph$: TPP
$R^1 = Me$; $R^2 = Ph$: TMP
$R^1 = R^2 = Me$: TMM

TPP (3, 4) is voltametrically reduced in ACN solution, in two successive peaks, to a radical anion and to a dianion at ca. −0.8 V (vs. Ag^+ (0.1 M ACN) / Ag), while **TPPH·OEt** in EtOH presents two reduction peaks at ca. −1.7 and −1.9 V.

In this work, the EtOH addition reactions and the electroreduction properties of the related compounds 3-methyl-4-phenyl-1,2,5-thiadiazole 1,1-dioxide (**TMP**) and 3,4-dimethyl-1,2,5-thiadiazole 1,1-dioxide (**TMM**) are studied in ACN and in EtOH solution and compared with those of **TPP**. Interesting differences related to the presence of a methyl group bonded to a very electron-deficient carbon atom are observed.

Experimental

TMP and **TMM** were synthesized, purified, and characterized according to published procedures (5). Standard methods of purification were used for ACN and EtOH solvents.

^1H and ^{13}C NMR spectra were measured with a Bruker 200 MHz instrument.

Conventional cyclic voltammetry techniques were employed. A L.Y.P. M2 potentiostat, a 3-module L.Y.P. sweep generator, and a Houston Omnigraphic 2000 pen recorder were used.

Voltammetric experiments were performed in an undivided, gas-tight, glass cell swept by purified nitrogen. The cell was kept in a dry glove box, where all solution preparation and other experimental manipulations were made. The reference electrode (r.e.) was Ag^+ (0.1 M ACN)/Ag. It was separated from the cell solution by a porous-glass plug. A 2 cm^2 Pt foil was the counter electrode and the working electrode (w.e.) was a Teflon encapsulated vitreous carbon disk of 0.074 cm^2.

Bulk electrolysis experiments were performed in a divided cell. The anodic and cathodic compartments were separated by a sintered glass plate. The cathode was a vitreous carbon rod (0.3 cm diameter and 1.5 cm length) and the anode was a 8 cm^2 Pt foil. The reference and the working electrode described above for cyclic voltammetry were included in the cathodic compartment and were used to measure the concentration of the substrate at convenient intervals during the electrolysis.

Results and discussion

(a) TMP

Voltammetric and bulk electrolysis results in ACN solution

The results of typical voltammetric experiments performed with solutions of **TMP** in ACN are shown in Fig. 1*a* and *b*. Published results corresponding **TPP** are also included in Fig. 1*c* for comparison. As can be observed, under the experimental conditions of Fig. 1*a*, **TMP** presents two redox couples (Ic/Ia; IIc/IIa), which, as in the case of **TPP**, can be assigned to the charge transfers:

$\mathbf{TMP} + e = \mathbf{TMP}^{\bullet-}$ Ic/Ia E_1

$\mathbf{TMP}^{\bullet-} + e = \mathbf{TMP}^{2-}$ IIc/IIa E_2

Fig. 1. Cyclic voltammograms, current function vs. potential, for **TMP** (at selected low and high experimental concentration) and for **TPP**. ACN solvent; 0.25 M $NaClO_4$ supporting electrolyte; vitreous carbon disk w.e.; Ag^+(0.1 M ACN)/Ag r.e.; $v = 0.2$ V s^{-1}. (*a*) **TMP**: 1.06 mM; (*b*) **TMP**: 13.7 mM; (*c*) (····) **TPP**: 1.51 mM.

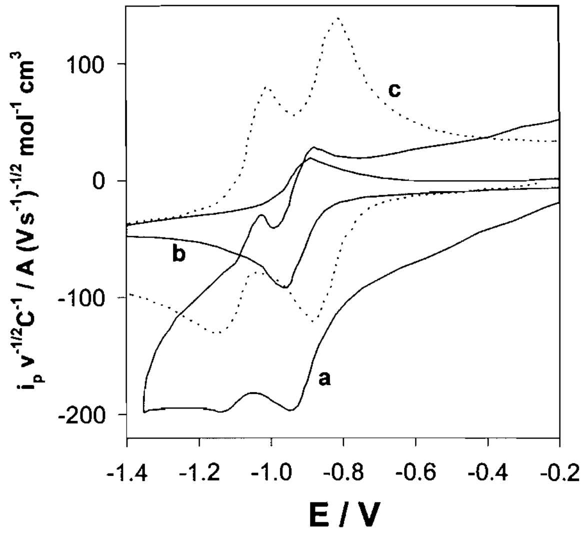

The first couple is clearly observed under all experimental conditions. The second couple (IIc/IIa) is always less intense and less well defined than the first. It is distinctly observed at low concentrations and high sweep rates, but its current intensity decreases at the higher experimental concentrations. Under the conditions of Fig. 1*b* it is no longer observable. This behavior, although less pronounced, was also observed with **TPP** and was related to interactions of the dianion of **TPP** with the cations of the supporting electrolyte and to adsorption processes (4). Only the processes related to the first couple will be studied in this work.

The current function of the cathodic peak (Ic) of the first couple does not change appreciably with concentration (in the range 1.06–37.7 mM, $i_p(\mathrm{Ic})\ v^{-1/2}\ C^{-1}/A\ (\mathrm{V\ s^{-1}})^{-1/2}\ (\mathrm{mol\ cm^{-3}})^{-1} = 83 \pm 6$). The diffusion coefficient, calculated with the equation for a reversible voltammetric wave, is 1.7×10^{-5} cm^2 s^{-1}, which is similar to that found for **TPP** (1.2×10^{-5} cm^2 s^{-1}).

Controlled potential electrolysis experiments at −0.9 V in ACN solvent were run with **TMP** initial concentrations ($[\mathbf{TMP}]_0$) of 21 and 2.2 mM. A duplicate electrolysis experiment with 2.2 mM **TMP** in which water (1.55 M) was added to the ACN solvent was also performed. All three experiments were coincident, within the experimental error (Fig. 2), indicating that *ca.* 0.4 electrons/mol **TMP** are consumed in the bulk electrolysis.

Fig. 2. Bulk electrolysis of **TMP** in ACN solution. Number of moles of electrons vs. relative concentration of **TMP** as measured through the voltammetric current intensity of peak Ic at several intervals during the electrolysis. $[\mathbf{TMP}]_0$: ∇:21 mM; ○:2.2 mM; ●:2.2 mM + 1.55 M water.

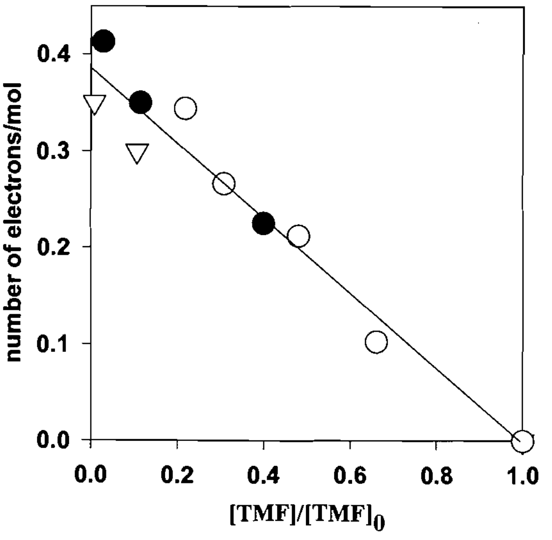

From the very beginning of the electrolysis experiments, the catholyte solution develops a dark red-brown color that originates near the cathode and increases in intensity as the electrolysis progresses. The color intensity decreases and turns yellowish on exposure of the electrolyzed solution to air. Thin-layer chromatographic analysis of the solution at the end of the experiments reveals a complex mixture. Initial efforts to isolate the components have been unsuccessful, but our work in this direction continues in connection with additional studies on the homogeneous reaction kinetics of **TMP**.

The first charge transfer for **TMP** takes place at a more negative potential than that of **TPP** ($E_{\mathrm{pIc[TPP]}} - E_{\mathrm{pIc[TMP]}} \cong 0.16$ V). This can be related to structural characteristics of the substrates and the radical anions formed.

van der Waals molecular models and X-ray crystal studies of both compounds (6) show that the two phenyl rings of **TPP** cannot be accommodated in the plane of the heterocycle (**TPP** dihedral angles: phenyl–phenyl = 51.9°; phenyl–heterocycle = 34.2 and 41.4°), and that the methyl group in **TMP** hinders the planar disposition of the phenyl ring and the heterocycle to a very similar extent (**TMP** dihedral angle: phenyl–heterocycle = 40.9°). It is reasonable to suppose that the electron transferred to the substrates to form the radical anions should favor a location associated with an electron-deficient heterocyclic carbon atom bonded to a phenyl group (because of charge dispersal reasons). Since more stabilization energy will be gained by delocalizing the additional electron, the phenyl ring involved should be more in the plane of the thiadiazole ring than in that of the parent neutral compound. This can be achieved in **TPP** by the concerted rotation of both rings, but it is not possible in **TMP**.

The peak current intensity ratio ($R_i = i_{\mathrm{pIa}}/i_{\mathrm{pIc}}$) of the first couple is always smaller than unity and decreases when the cathodic switching potential is made increasingly negative. R_i is also a function of **TMP** concentration and sweep rate as shown in Fig. 3 for a constant switching potential (−1.04 V) that does not include the second couple.

Fig. 3. Influence of sweep rate and concentration in the ratio of anodic to cathodic peak current intensity (R_i) of the first voltammetric couple of **TMP** for a constant switching potential $E_s = -1.04$ V; ACN solvent; 0.25 M $NaClO_4$ supporting electrolyte; vitreous carbon disk w.e.; Ag^+(0.1 M ACN)/Ag r.e. [**TMP**]: ○:37.7; □:13.7; Δ:9.13; ∇:3.61; ◇:1.06 mM. The dotted line represents the result of a digital simulation for a radical–substrate reaction mechanism with rate constant $k = 3 \times 10^2$ M^{-1} s^{-1} (see also Fig. 6).

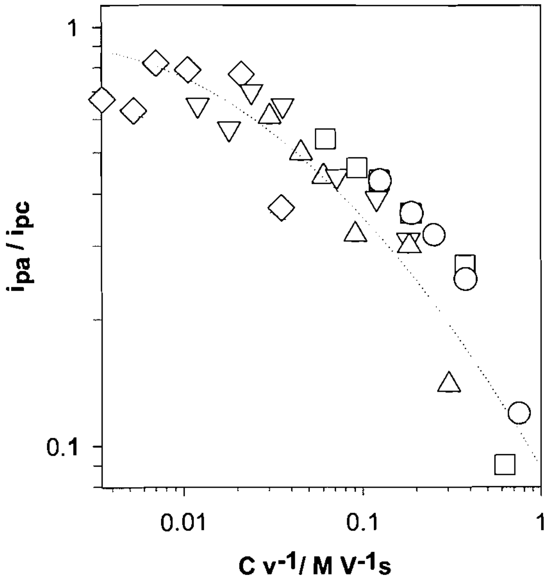

The data shown in Fig. 3 suggest the consumption of $\mathbf{TMP}^{\cdot-}$ by a second-order reaction that, at a constant sweep rate; causes the decrease of R_i with increasing concentration, reflecting the increase in reaction rate; conversely, R_i tends to increase up to unity when the time window is decreased through an increase of the sweep rate. The dotted line in Fig. 3 represents the results of a digital simulation for a radical–substrate second-order reaction, which is justified in the following:

The mechanism of the reaction can be further characterized through the slopes $\delta E_p/\delta \log(v)$ and $\delta E_p/\delta \log[\mathbf{TMP}]$. Figure 4 shows the dependence of the potential of peak Ic with sweep rate at several **TMP** concentrations. A 28.5 mV/dec (r = 0.986; 9 points) $\delta E_p/\delta \log(v)$ slope is observed for [**TMP**] = 37.7 mM for the whole range of experimental sweep rates. At lower concentrations the slope is similar for the lower sweep rates, but $\delta E_p/\delta \log(v)$ tends to zero when the sweep rate is increased. Finally, for [**TMP**] = 1.06 mM, the peak potential does not change with sweep rate.

The $\delta E_p/\delta \log[\mathbf{TMP}]$ slope is shown in Fig. 5 for sweep rates of 0.005, 0.01, and 0.02 V s^{-1}, in the concentration range in which irreversible voltammetric signals are observed. The observed slopes are 43, 34, and 29 mV/dec, respectively. Given the observed $\delta E_p/\delta \log(v)$ slope, the expected $\delta E_p/\delta \log[\mathbf{TMP}]$ slopes for the well-known simple second-order reaction mechanisms are either 19.7 or 29.6 mV/dec (7).

Obviously the slopes are closer to 29.6 mV/dec, which corresponds to a radical–substrate reaction. The discrepancy might be due to a more complex mechanism or it may be an artifact due to the complex reaction observed in the controlled potential electrolysis experiments. This seems reasonable since the slope departs increasingly from the expected value at decreasing sweep rates.

If the radical–substrate reaction is accepted as the dominant mechanism, a rate constant, k_1, for the reaction:

[1] **TMP**$^{\cdot-}$ + **TMP** = products

can be calculated from the sweep rate (v_i) at which the E_p vs. log ($C\,v^{-1}$) slope changes (7), or, as is shown in Fig. 6, a more detailed view of the fitness of the radical–substrate mechanism can be furnished by a digital simulation that takes into account the electron transfer E_1, followed by reaction [1] and a fast electroreduction of the product (i.e., $E^0_{(\mathrm{product})} \gg E_1$). The simulation results, indicated in Fig. 6 with a solid line, correspond to $k_1 = 3 \times 10^2\,\mathrm{M}^{-1}\,\mathrm{s}^{-1}$.

The methyl protons of **TMP**, being bonded to a very electron-deficient carbon atom, are weakly acidic. Thus, the radical–substrate reaction might consist of a proton transfer (reaction [1]). The reaction will also be driven forward by the fast electroreduction of the radical **TMPH**$^{\cdot}$ at $E_3 > E_1$.

Anions of the 3-oxo derivatives of 1,2,5-thiadiazole 1,1-dioxides are well known (1). Anion **I**$^-$ has a similar structure although it must be much less stable. Follow-up reactions involving anion **I**$^-$ such as an aldolic-type condensation (reaction [2]), are also possible and have been observed in related compounds (8). The consumption of the substrate by the follow-up reactions can account for the reduced number of electrons per mole observed in the electrolysis experiments.

Voltammetric results in EtOH and ACN/EtOH solutions

The voltammetric results in EtOH solvent are presented in Fig. 7*a* (solid line). The results obtained with **TPP** (4), which have already been discussed, are included for comparison (Fig. 7*a*; dotted line). As was the case for **TPP**, the EtOH molecule adds to one of the C=N double bonds of **TMP** to form a thiadiazoline:

[3] **TMP** + EtOH = **TMPH·OEt**

which is voltammetrically reduced in two peaks (IIIc and IVc) that are very similar to those found with the **TPP** substrate.

[1*a*]

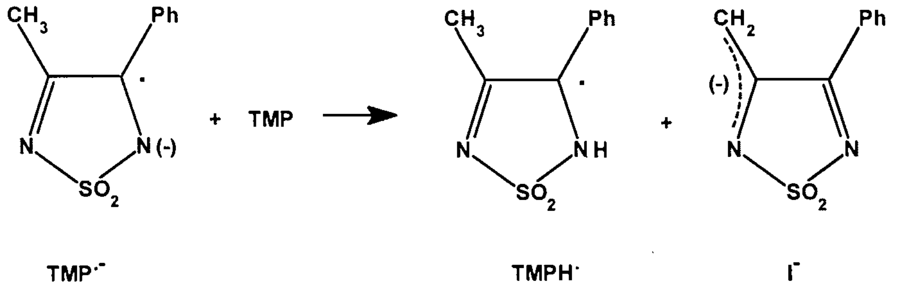

E_3 TMFH$^{\cdot}$ + e$^-$ $\rightleftharpoons$ TMFH$^-$

[2]

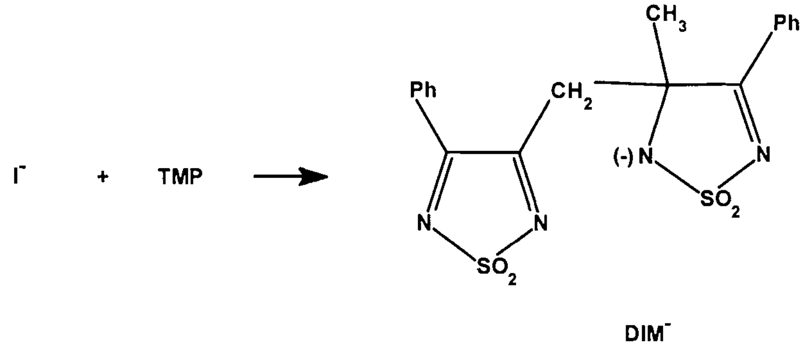

When EtOH is added to ACN solutions of **TMP**, the voltammograms evolve in time in essentially the same way as was observed for **TPP** (4), that is, the **TMP** voltammetric peaks are observed initially and peak IVc at −1.94 V starts to develop (Fig. 7*b*, solid line). This is followed by the decrease and disappearance of peak IIc, while peak IVc increases. After the disappearance of peak IIc, peak IIIc appears at ca. −1.65 V and grows while the current intensity of peak Ic decreases

Fig. 4. Peak potential for the first couple of **TMP** (E_pIc), vs. Ag^+ (0.1 M ACN)/Ag, as a function of sweep rate for several concentrations of **TMP** in ACN solution; 0.25 M $NaClO_4$ supporting electrolyte; vitreous carbon disk w.e. [**TMP**]: ○:37.7; □:13.7; Δ:9.13; ∇:3.61; ◇:1.06 mM. Solid line through ○ is a least-squares regression (*r*: 0.986; slope: 28.5 mV/dec); solid line through ◇ is the average of peak potentials for [**TMP**] = 1.06 mM (E_p (mean) = −0.933 V).

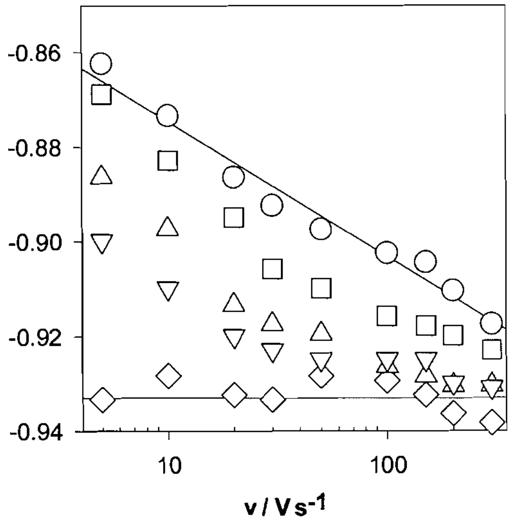

Fig. 5. Peak potential for the first couple of **TMP** (E_pIc), vs. Ag^+(0.1 M ACN)/Ag, as a function of the concentration of **TMP** for several sweep rates in ACN solution; 0.25 M $NaClO_4$ supporting electrolyte; vitreous carbon disk w.e. Sweep rates: ○:0.005; ●:0.010; Δ:0.020 V s^{-1}. The concentration ranges from the highest experimentally used to the lowest in which irreversible peaks are still observed at each sweep rate. Solid lines are least-squares regressions with the following slopes and regression coefficients: 43 mV/dec; *r* = 0.975 (8 points); 34 mV/dec, *r* = 0.941 (7 points); Δ:29 mV/dec, *r* = 0.943 (5 points).

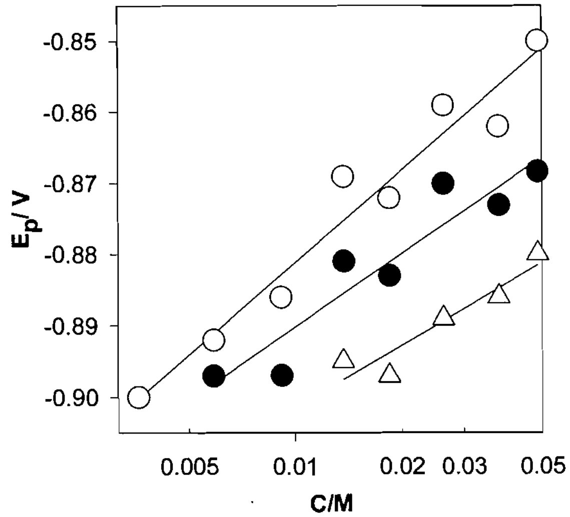

slightly. Finally an equilibrium voltammogram is obtained (Fig. 7*b*, dotted line).

Fig. 6. Peak potential for the first couple of **TMP** (E_pIc), vs. Ag^+ (0.1 M ACN)/Ag as a function of the ratio of **TMP** concentration to sweep rate in ACN solution. [**TMP**]: ○:37.7; □:13.7; Δ:9.13; ∇:3.61; ◇:1.06 mM; (—): digital simulation with $k = 3 \times 10^2\ M^{-1}\ s^{-1}$.

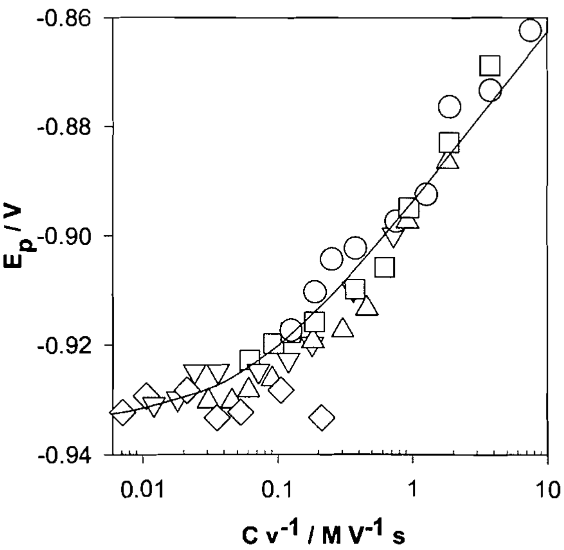

Fig. 7. Cyclic voltammograms at 0.1 V s^{-1} of: (*a*) **TMP** in ethanol; (*b*) in ACN–EtOH, 7.5 wt.% EtOH. (*a*) (—): 5.05 mM **TMP** in EtOH; (· · ·): 3.16 mM **TPP** in EtOH, included for comparison. (*b*) Voltammograms of 3.65 mM **TMP** in ACN–EtOH, 7.5 wt.% EtOH. (—): 15 min after solution preparation; (· · ·): equilibrium voltammogram, 10 days after solution preparation.

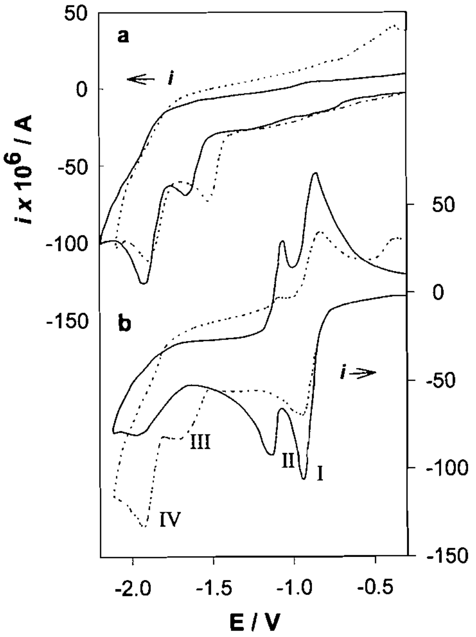

The time evolution described can be interpreted by a reaction mechanism essentially identical to that proposed for **TPP** in ACN–EtOH solvent mixtures. Thus at peak I (Fig. 7*b*) **TMP** is reduced and the radical anion formed reacts

Table 1. Experimental voltammetric results and calculated values of the equilibrium constant K_{TMP} (uncontrolled room temperature, ca. 20°C) for the reaction: **TMP** + EtOH = **TMPH·OEt**.

$[EtOH]_0$/M	$[TMP]_0$/mM	v/(V s^{-1})	i_p(Ic)/(μA)	i_p(IIIc)/(μA)	K_{TMP}/M^{-1}
2.96	3.60	0.10	27.0	27.5	1.03
1.30	3.65	0.10	56.0	25.0	1.46
2.83	3.75	0.10	18.0	25.0	1.33

with EtOH. The product is further reduced at a potential $E_3 > E_1$.

$$\mathbf{TMP}^{\cdot -} + \text{EtOH} = \mathbf{TMPH}^{\cdot} + \text{EtO}^- \qquad C_4$$

$$\mathbf{TMPH}^{\cdot} + e^- = \mathbf{TMPH}^- \qquad E_3$$

If some **TMPH·OEt** has been formed through reaction [3], it reacts with the strong EtO^- base:

$$\text{EtO}^- + \mathbf{TMPH{\cdot}OEt} = \text{EtOH} + \mathbf{TMP{\cdot}OEt}^- \qquad C_5$$

The remaining $\mathbf{TMP}^{\cdot -}$ is further reduced at E_2 (peak IIc). The anions produced at E_3 and C_5 ($\mathbf{TMPH}^-$ and $\mathbf{TMP{\cdot}OEt}^-$) are further reduced at peak IVc. If some **TMPH·OEt** remains it will be reduced at peak IIIc:

$$\mathbf{TMPH{\cdot}OEt} + e^- = \mathbf{TMPH{\cdot}OEt}^{\cdot -} \qquad E_4$$

$$\mathbf{TMPH{\cdot}OEt}^{\cdot -} = \mathbf{TMPH}^{\cdot} + \text{EtO}^- \qquad C_6$$

The $\mathbf{TMPH}^{\cdot}$ formed in C_6 will be immediately reduced to $\mathbf{TMPH}^-$ (E_3).

Thus, once peak IIc is no longer observed, peak Ic will be a two-electron $E_1C_4E_3$ peak, and its intensity will depend on the **TMP** concentration. Likewise, peak IIIc will be a two-electron $E_4C_6E_3$ peak and its current intensity will depend on the actual **TMPH·OEt** interfacial concentration, i.e., its bulk concentration minus the depletion caused by reaction C_5.

The equilibrium constant of reaction [3], k_{TMP}, can be calculated using the same relation of peak intensities used for **TPP** (4), specifically:

$$K_{TMP} = \frac{[\mathbf{TMPH{\cdot}OEt}]}{[\text{EtOH}][\mathbf{TMP}]}$$

$$= (2 \times \{i(\text{IIIc}) + i(\text{Ic})/2\}/[\text{EtOH}]_0 \times i(\text{Ic}))$$

The experimental peak intensities and calculated K_{TMP} for several EtOH concentrations are shown in Table 1.

The equilibrium constant K_{TMP} was also calculated using UV spectral measurements and a Hildebrand-type equation, as has been done with **TPP**. The details will be reported elsewhere, but the spectroscopically measured value, 1.4 M^{-1} at 25.0°C, agrees with the voltammetric value of Table 1.

The resonance of the heteronuclear methyl substituent in ^{13}C NMR measurements of **TMP** is, in benzene-d_6 solution, observed at δ = 17.6 ppm, and in methanol-d_4 solution at δ = 26.5 ppm. The direction and magnitude of the observed shift (Δδ = 8.9 ppm) is in agreement, according to the additivity rules for ^{13}C chemical shifts (9), with the addition of MeOH to the C=N double bond on the methyl "side" of the molecule. Thus the thiadiazoline **TMPH·OEt** has the structure:

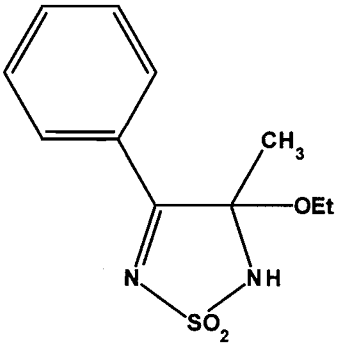

TMP.EtOH

It can be observed that the π-system of **TMPH·OEt** is very similar to that of **TPPH·OEt**, This rationalizes the above-mentioned similarities between the voltammetric responses of both thiadiazolines. The similarity of the delocalization energy increment in going from the thiadiazoles to the thiadiazolines is also shown in the values of the equilibrium constants of the EtOH addition reactions. Thus, k_{TPP} is approximately two times larger than K_{TMP}, as can be expected if only symmetry factors are important.

(b) TMM

Voltammetric results for TMM in ACN solutions

The cyclic voltammetry of **TMM** in ACN solutions results in a single, diffusional, totally irreversible voltammetric peak at ca. −1.00 V under all experimental conditions. The peak shifts cathodically 30 mV/dec of sweep rate and its potential does not depend on the substrate concentration. Its current function ($i_p\, v^{-1/2}\, C^{-1}$) decreases slightly but steadily with the increase in concentration from 71 A V^{-1} $s^{1/2}$ mol^{-1} cm^3 at 1.01 mM, to 66 at 11.2 mM, and then drastically to 40 A V^{-1} $s^{1/2}$ mol^{-1} cm^3 at the highest concentration used (17.1 mM). This is apparently related to an increase in the rate of fouling of the electrode with increasing concentration. In effect, the second voltammetric cycle at all concentrations shows a decrease in current intensity that increases in magnitude when the concentration is increased. The current is restored to its first-cycle value when the electrode surface is cleaned.

These results suggest a one-electron charge transfer followed by a fast chemical reaction and allow the calculation of a diffusion coefficient, $D_{(\mathrm{TMM})} = 1.2 \times 10^{-5}$ cm^2 s^{-1}, which is similar to those of **TPP** and **TMP**. Thus, as seems reasonable because of the lack of delocalization possibilities, the radical anion of **TMM** is unstable.

Voltammetric results for TMM in EtOH solutions

As found for **TPP** and **TMP**, the current intensity of the voltammetric peak of **TMM** in ACN–EtOH solvent mixtures decreases initially with time and reaches a stable equilibrium value that is lower the higher the EtOH concentration. No new peaks are observed and, since a thiadiazoline is formed according to the NMR evidence given below, it must be concluded that the 3,4-dimethyl thiadiazoline can not be reduced at potentials more anodic than the solvent cutoff.

The ^{1}H NMR spectrum of **TMM** provides evidence of an addition reaction of EtOH to one of the C=N double bonds of **TMM**. A single methyl signal at δ = 2.63 ppm is observed in ACN-d_3, while two methyl signals are present in ethanol-d_6, at δ = 2.35 ppm (assigned to the methyl on the unsubstituted side) and 1.68 ppm (assigned to the methyl on the ethoxyl-substituted side). In ACN-d_3–ethanol-d_6 solvent mixtures the original substrate methyl signal is also observed at 2.62 ppm. A study (at an uncontrolled room temperature of *ca.* 20°C) of the relative intensities of these three signals in ACN-d_3–ethanol-d_6 solvent mixtures with 13.3, 30.0, and 60.0 wt.% ethanol-d_6 allowed an evaluation of $K_{\mathrm{TMM}} = 0.3$ M^{-1} (individual measurements were 0.26, 0.30, and 0.32 M^{-1}, respectively).

UV–VIS spectroscopic techniques cannot be used to study the addition reaction, since **TMM** presents only terminal absorption at $\lambda < 300$ nm, but an equilibrium constant can be estimated from voltammetric experiments if the equilibrium peak current intensity (corrected for the viscosity change of the solvent by means of independent measurements of the intensity of the ferrocene couple in the same solvent mixtures, as already described (4)) of the **TMM** peak in ACN–EtOH solvent mixtures is taken as a measure of its equilibrium concentration.

Four voltammetric experiments in ACN–EtOH solvent mixtures with 9.9, 21, 42, and 75.6 wt.% EtOH were performed. The K_{TMM} values (uncontrolled room temperature, ca. 20°C) calculated were 0.16, 0.15, 0.18, and 0.20 M^{-1}. Due to the assumptions involved, this estimate of K_{TMM} can be considered to be in reasonable agreement with the more direct NMR experiments.

Influence of the addition of acids in the voltammetry of TMP and TMM in ACN, EtOH, and mixed ACN–EtOH solvents

TMP or TMM in ACN + acid: Experiments in which several concentrations of dry trifluoracetic acid (TFAcH) were added to ACN solutions of **TMP** or **TMM** were performed. In both cases a kinetic prepeak (ppIc), anodic to the first charge transfer, developed when less than equimolecular quantities of acid were added. The prepeak current intensity increased with increasing relative concentrations of acid and finally replaced the original peaks of the substrate when the relative concentration of acid ([TFAcH]/[**TMP**] or [TFAcH]/[**TMM**]) was 2 or greater. The current intensity of the prepeak under these conditions is twice that of the original peak Ic of the substrate.

At low ratios of acid to substrate concentration, the prepeak can be interpreted as the reduction of the substrate, followed by protonation of the radical anion, i.e., for **TMP**:

$$\mathbf{TMP} + e^- = \mathbf{TMP}^{\bullet-} \qquad E_1$$

$$\mathbf{TMP}^{\bullet-} + 2\,\mathrm{TFAcH} = \mathbf{TMPH}^{\bullet} + (\mathrm{TFAc})_2\mathrm{H}^- \qquad C_7$$

The **TMPH**$^{\bullet}$ radical can be further reduced to the anion and protonated to the thiadiazoline (**TMPH**$_2$) or it can disproportionate to form **TMPH**$_2$ and regenerate the substrate, which will be reduced at E_1.

Reaction C_7 includes the well-known homoconjugation reaction of anions in ACN (10).

TMP, TPP, or TMM in ETOH + acid: Similar results are obtained if TFAcH is added to solutions of **TPP** or **TMP** in EtOH solvent. A prepeak (ppIIIc) develops and its associated current intensity increases on increasing the acid concentration. The original peaks (IIIc and VIc, Fig 7*a*) are completely replaced by the prepeaks (which double the current intensity of each original peak) when the acid concentration is more than twice that of the substrate. The prepeaks are interpreted as above by equations similar to E_1 and C_7, in which **TMP** is replaced by **TMPH·OEt**.

As already discussed, the voltammetric electroreduction of **TMMH·OEt** takes place beyond the solvent potential cutoff. The addition of TFAcH to solutions of **TMM** in EtOH solvent does not cause the appearance of new voltammetric peaks.

TMP or TPP in mixed ACN–EtOH + acid: In mixed ACN–EtOH solvents to which TFAcH (with ratios [TFAcH]/[**TMP**] or [TFAcH]/[**TPP**] ca. 4) has been added, it is possible to record voltammograms in which only both prepeaks, ppIc and ppIIIc, are observed.

Since ppIc responds to the concentration of the thiadiazole ([**TPP**] or [**TMP**]) and ppIIIc to the concentration of thiadiazoline ([**TPPH·OEt**] or [**TMPH·OEt**]), it follows that equilibrium constants for the EtOH addition reactions to **TPP** and **TMP** (K_{TPP} and K_{TMP}) can be measured voltammetrically in these mixed solvent solutions. K_{TMP}, for example, can be expressed as:

$$K_{\mathrm{TMP}} = \frac{[\mathbf{TMPH{\cdot}OEt}]}{[\mathrm{EtOH}][\mathbf{TMP}]} = \frac{i(\mathrm{ppIIIc})/v^{1/2}}{\{i(\mathrm{ppIc})/v^{1/2}\} \times [\mathrm{EtOH}]}$$

The experimental results are given in Table 2. The calculated equilibrium constants for **TMP** and **TPP** agree with those calculated from the complex mechanism in mixed ACN–EtOH solvents for **TMP** (above) and **TPP** (4).

Acknowledgments

This work was financially supported by the Consejo Nacional de Investigaciones Científicas y Técnicas (CONICET), the Comisión de Investigaciones Científicas de la Provincia de Buenos Aires (CIC Pcia. Bs.As.), and the University of La Plata (UNLP), Facultad de Ciencias Exactas, Departamento de Química. M.V.M and J.A.C. are researchers of CONICET and UNLP, E.J.V. is researcher of CIC Pcia. Bs.As and UNLP. The authors acknowledge the assistance of Prof. Dr. E.G. Gros (UMyMFOR, Universidad de Buenos Aires, CONICET) for the NMR spectral measurements.

Table 2. Experimental voltammetric results for (*a*) **TMP** and (*b*) **TPP** in mixed ACN–EtOH solvents with added trifluoroacetic acid (TFAcH). Calculated values for the equilibrium constants of the EtOH addition reactions (uncontrolled room temperature, ca. 20°C). $i_p/v^{1/2}$ values are the mean of seven values measured at sweep rates between 0.01 and 0.5 V s^{-1}.

[**TMP**]/mM	[TFAcH]/mM	[EtOH]/M	i(ppIc)/$v^{1/2}$	i(ppIIIc)/$v^{1/2}$	K_{TMP}
3.88	9.10	0.59	294	243	1.40
3.93	9.10	1.63	157	397	1.55
3.85	9.10	3.30	95.9	484	1.53

[**TPP**]/mM	[TFAcH]/mM	[EtOH]/M	i(ppIc)/$v^{1/2}$	i(ppIIIc)/$v^{1/2}$	K_{TPP}
4.23	10.4	1.66	76.6	403	3.16
4.24	10.4	2.57	63.3	618	3.80
4.19	10.4	3.32	48.9	546	3.36
4.23	10.4	3.40	42.7	439	3.02
4.20	10.4	4.17	50.0	621	2.98

References

1. V.J. Aran, P. Goya, and C. Ochoa. Adv. Heterocycl. Chem. **44**, 81 (1988)
2. M.V. Mirífico, J.A. Caram, E.J. Vasini, and J.E. Sicre. J. Phys. Org. Chem. **6**; 341 (1993).
3. M.V. Mirífico, J.A. Caram, and E.J. Vasini. Electrochim. Acta, **36**, 167 (1991).
4. J.A. Caram, M.V. Mirífico, and E.J. Vasini. Electrochim. Acta, **39**, 939 (1994).
5. J.B. Wright. J. Org. Chem. **29**, 1905 (1964).
6. E.E. Castellano, O.E. Piro, M.D. Glossman, J.A. Caram, and E.J. Vasini. Proceedings of the XVIII Encontro Nacional de Física da Materia Condensada. Caxambú (MG), Brazil, June 1995.
7. C.P. Andrieux, L. Nadjo, and J.M. Saveant. J. Electroanal. Chem. **42**, 223 (1973).
8. P. Goya, A. Martinez, C. Ochoa, M. Stud, and M. L. Jimeno. Tetrahedron, **41**, 3105 (1985).
9. E. Pretsch, T. Clerc, J. Seibl, and W. Simon. Tabellen zur strukuraufklärung organischer verbindungen mit spektroscopishen methoden. Springer Verlag, Berlin. 1976.
10. J.F. Coetzee and G.R. Padmanabhan with G.P. Cunningham. Talanta, **11**, 93 (1964).